3.4 Simple Radiative-convective Models

Two simple models can explain the gross features of the vertical profile of temperature. The first model uses radiative equilibrium; however, this model develops super adiabatic lapse rates in the lower atmosphere. The super adiabatic lapse rates are removed by simple convective adjustments in the second model. Though crude, these models can be used to illuminate (a) why the atmospheric lapse rates vary with altitude, including the presence of a tropopause, (b) why the height of the tropopause varies with latitude, and (c) why the lapse rates vary with latitude. Fully explaining these three variations requires further embellishment: incorporating heat transports by large-scale circulations. To keep the discussion as simple as possible, important and complex effects due to clouds are ignored. Hence, the discussion is not intended to be complete. Several books (e.g., Paltridge and Platt, 1976) treat radiation and radiative convective models with greater care and in greater depth than the scope of this book allows.
The original derivation of a radiative balance model for the atmosphere is attributed to Emden (1913). The standard development can be found in both editions of Goody and Yung (1989). The discussion here is streamlined and based upon comprehensible works by Houghton (1977) and Paltridge and Platt (1976).

Absorption of radiation along a vertical path may be described by Lambert's law or Bouguer's law (Tagirov and Tagirov, 1997), Beer's law, or a combination of these names. The different names arise from expressing the attenuation as a function of distance or absorber concentration. Applied to the atmosphere, there is an additional consideration of scattering that will be ignored here.

Lambert's law states that as a beam of radiation travels through a slab of atmosphere it will be absorbed at a rate proportional to (a) the thickness of the slab dz, (b) the angle of the beam from to normal to the slab ϕ, (c) the density of the absorber ρ_a, and (d) the intensity of the incident beam of radiation I. The incoming radiation I could be parallel beam irradiance or radiance. The path length through the absorber is thus $dX = \sec\phi\, dz$, as shown in Figure 3.15a. Thus the loss of incident radiation per unit horizontal cross-sectional area as it passes through the absorber is:

$$dI = -I\, k_a\, \rho_a\, dX \tag{3.18}$$

In (3.18) k_a is the mass extinction (absorption) coefficient.

Radiation may be diffuse or parallel beam. Parallel-beam radiation describes the solar radiation reaching the Earth to a good approximation. The Earth and its atmosphere emit

radiation in all directions, so one must treat terrestrial radiation as diffuse. The terrestrial radiation could be treated as radiance or as irradiance from a hemisphere (upward or downward).

Since the Sun is very far away (compared to its radius), solar radiation reaching the earth can be treated as parallel-beam radiation to high accuracy. *In that case, I* is the solar *irradiance*. The solar radiation $I(z)$ is directed downward (z *decreasing*) so that $I(z)$ must increase with height. Integrating (3.18) in the vertical from height z to ∞ gives the irradiance arriving at level z.

$$I(z) = I_0 \exp\left(-\sec\phi \int_z^\infty k_a \, \rho_a \, dz \right) \tag{3.19}$$

where I_0 is the intensity of incident radiation at the top of the atmosphere. The integral

$$O_a = \int_z^\infty k_a \, \rho_a \, dz \tag{3.20}$$

Defines the quantity O_a commonly known as the *optical depth* for absorber a. (Some authors use the optical *path*, which is usually defined as $O_a \sec\phi$.) The optical depth stretches the vertical coordinate as a function of the amount of absorber.

The atmosphere emits as well as absorbs radiation. The emission, E_{ei}, is not parallel-beam radiation but is diffuse. The emission is a function of solid angle and is termed *radiance*. Irradiance, I_{ei}, is calculated by integrating the diffuse radiance over all solid angles. One may approximate the atmosphere by plane parallel layers, each indexed by a subscript. When radiance is isotropic, then the irradiance I_{ei} is related to radiance by a factor of π. For all directions and using radiance E_{ei} emitted from layer i, then

$$\int_0^{2\pi} \int_0^{\pi} E_{ei} \sin\phi \, d\phi \, d\lambda = \int_0^{\pi} E_{ei} \, d\omega = 4\pi \, E_{ei} = 4 I_{ei} \tag{3.21}$$

where $d\omega$ is an element of solid angle, ϕ is the angle of incidence relative to the direction normal to the unit horizontal area (Figure 3.15) and λ is the azimuth angle. The second step in (3.21) assumes that the E_{ei} from layer i is isotropic. From the Stefan-Boltzmann law, irradiance is proportional to the temperature (T_i) of the emitter ($I_{ei} = \sigma T_i^4$).

The net radiative transfer dI_i through the slab i is the difference between the radiation absorbed by the slab and the radiation emitted by the slab. *Thus*

$$dI_i = -I_i \, k_a \, \rho_a \sec\phi \, dz + E_{ei} \, k_a \, \rho_a \sec\phi \, dz = dO_a \left(E_{ei} - I_i \right) \tag{3.22}$$

Use is made of $dO_a = -k_a \, \rho_a \, dz$ where the sign reversal is because dz and dO_a increase in opposite directions. Use is also made of Kirchoff's law by using the same k_a in both terms on the right hand side of (3.22). Rearranging (3.22) obtains this radiative transfer equation

$$\cos\phi \frac{dI_i}{dO_a} = I_i - E_{ei} \tag{3.23}$$

Since (3.23) holds for a particular path, the next step is to collapse the angular variation into components (up or down) in the vertical.

At this point absorption of solar radiation is no longer considered, but instead absorption of terrestrial radiance is used. Hence I in equations (3.22) and (3.23) will be incident radiance E_I. Furthermore, (3.23) is a general expression for how radiance changes with optical depth and the subscript 'i' is dropped in favor of vertical integration later. Hence,

$$\cos\phi \frac{dE_I}{dO_a} = E_I - E_e \tag{3.24}$$

The use of notation E_I in (3.24) is useful since E_I is radiance in a single direction at present.

To collapse the directional dependence, one introduces some definitions. The first definition uses a cosϕ weighting to obtain the *net* vertical flux of radiant energy I_F (an irradiance) from the radiant energy flux, E_I (a radiance). Hence,

$$I_F \equiv \int_0^{\pi} E_I \cos\phi \, d\omega \tag{3.25}$$

Second, define

$$E_I^{\omega} \equiv \frac{1}{4\pi} \int_0^{\pi} E_I \, d\omega \tag{3.26}$$

The E_I^{ω} is the "mean intensity" (Goody and Yung, 1989) or average radiance through a unit horizontal area from all angles integrated over a unit sphere. Next apply the 'method of moments' (Goody and Yung, 1989) which repeatedly applies the operator: $\cos^n\phi \, d\omega$ to the equation of transfer (3.24) and then integrates the resulting equation over solid angles of the unit sphere. The result is several equations that are related. The goal is to remove the troublesome $dE_I/d\tau$ term.

Multiplying (3.24) by $d\omega$ and integrating over all solid angles yields the n=0 moment equation

$$\begin{aligned} \int_0^{\pi} \cos\phi \frac{dE_I}{dO_a} d\omega &= \int_0^{\pi} E_I \, d\omega - \int_0^{\pi} E_e \, d\omega \\ \frac{dI_F}{dO_a} &= 4\pi E_I^{\omega} - 4\pi E_e^{\omega} = 4\pi E_I^{\omega} - 4I_e \end{aligned} \tag{3.27}$$

The second line uses (3.25) and (3.26); I_e is the irradiance of the layer as in (3.21). The second moment equation (n=1) is

$$\int_0^{\pi} \cos^2\phi \frac{dE_I}{dO_a} d\omega = \int_0^{\pi} E_I \cos\phi \, d\omega - \int_0^{\pi} E_e \cos\phi \, d\omega = I_F - \int_0^{\pi} E_e \cos\phi \, d\omega = I_F \tag{3.28}$$

The isotropy of E_e is used to obtain the last form.

A closure assumption is made that separates radiance E_I into upward E_U and downward E_D radiances. Radiant intensity E_I could vary with angle. Upward directed radiance comes from the Earth's surface and from atmospheric layers beneath layer i. Downward directed radiance comes from the layers above, and possibly from a source in outer space. Hence the upward could be notably different from the downward flux. Since cosϕ changes sign between upward and downward facing hemispheres, I_F could be the small difference between two large quantities. So, replacing dE_I/dO_a with its average value over all solid angles in (3.27) would not be wise. In contrast, the $\cos^2\phi$ factor in (3.28) is always positive, so it is more reasonable to replace dE_I/dO_a in (3.28) by its average value $\left(= 4\pi \, dE_I^{\omega} / dO_a\right)$. Making that substitution and integrating obtains

$$\begin{aligned} \int_0^{\pi} \cos^2\phi \frac{dE_I}{dO_a} d\omega &= \int_0^{\pi} \frac{dE_I^{\omega}}{dO_a} \cos^2\phi \, d\omega = \frac{dE_I^{\omega}}{dO_a} \int_0^{2\pi} \int_0^{\pi} \cos^2\phi \sin\phi \, d\phi \, d\lambda \\ &= \frac{dE_I^{\omega}}{dO_a} \left(\frac{-2\pi}{3}\right) \cos^3\phi \Big|_0^{\pi} = \left(\frac{4\pi}{3}\right) \frac{dE_I^{\omega}}{dO_a} = I_F \end{aligned} \tag{3.29}$$

Taking the derivative of (3.27) with respect to O_a obtains

$$\frac{d^2 I_F}{dO_a^2} = 4\pi \frac{dE_I^{\omega}}{dO_a} - 4\frac{dI_e}{dO_a} = 3I_F - 4\frac{dI_e}{dO_a} \tag{3.30}$$

A layer of air could be heated or cooled radiatively if there is a divergence of the radiant energy flux, I_F. Furthermore, horizontal divergence is essentially zero since horizontal differences of I_F can be assumed to be much smaller than vertical differences. Hence the divergence of I_F is given by dI_F/dO_a. If the atmosphere is in radiative equilibrium, then it is neither heating up nor cooling down. For the moment, ignore absorption of solar radiation in a layer. For any layer dO_a thick, the amount of energy entering that layer must equal the amount leaving that layer otherwise the layer heats up or cools down; that situation implies I_F is a constant in the vertical and that $dI_F/dO_a = 0$.

Radiative equilibrium with neglected horizontal variations reduces (3.30) to

$$3I_F = 4\frac{dI_e}{dO_a} \tag{3.31}$$

From partitioning E_I in (3.25)

$$I_F = \int_0^{\pi/2} E_U \cos\phi \, d\omega + \int_{\pi/2}^{\pi} E_D \cos\phi \, d\omega$$
$$= \int_0^{2\pi}\int_0^{\pi/2} E_U \cos\phi \sin\phi \, d\phi d\lambda + \int_0^{2\pi}\int_{\pi/2}^{\pi} E_D \cos\phi \sin\phi \, d\phi d\lambda = \pi\left(E_U - E_D\right) \tag{3.32}$$

Equation (3.32) means that I_F is the difference between the irradiance directed upward and the irradiance directed downward that must be eliminated for radiative balance. Figure 3.15d-f shows the geometry consistent with (3.32). *Since (i) no solar absorption by the air is included and (ii) the air cannot be heating up, then the difference I_F must be the same as the amount of solar radiation absorbed by the ground*. A second equation involving E_U and E_D is obtianed from (3.26)

$$E_I^{\omega} = \frac{1}{2}\left(E_U + E_D\right) \tag{3.33}$$

Use is made of the assumption that E_U and E_D are isotropic within their respective hemispheres. Eliminating E_U and E_I^{ω} from (3.32) and (3.33) by using (3.27)

$$0 = 4\pi E_I^{\omega} - 4I_e \tag{3.34}$$

Using (3.34) obtains

$$I_e\left(O_a\right) = \frac{I_F}{2} + \pi E_D \tag{3.35}$$

At the top of the atmosphere, E_D =0 (figure 3.15d), so

$$\sigma T_{sa}^4 = I_e\left(O_a = 0\right) = \frac{I_F}{2} \tag{3.36}$$

This equation defines the 'skin temperature' T_{sa} at the top of the atmosphere. Eliminating E_D and E_I^{ω} from (3.32) and (3.33) by using (3.27) obtains

$$I_e\left(O_a\right) = -\frac{I_F}{2} + \pi E_U \tag{3.37}$$

At the bottom of the atmosphere, the only contribution to E_U is from the Earth's surface (not the atmosphere, figure 3.15f) hence E_U can be expressed in terms of the surface temperature T_G. Hence

$$\sigma T_G^4 = I_G = I_e(at\ ground) = \pi E_U = I_e\left(O_{ab}\right) + \frac{I_F}{2} \tag{3.38}$$

The optical depth at the bottom of the atmosphere is O_{ab} and the irradiance from the Earth's surface is I_G. To obtain the atmospheric irradiance at other levels, one integrates (3.31) downward from O_a=0 to O_a using (3.36) and noting that I_F is constant.

$$\int_0^{O_a} dI_e = I_e(O_a) - I_e(0) = I_e(O_a) - \frac{I_F}{2} = \frac{3}{4} I_F O_a \qquad (3.39)$$

And thus

$$\sigma T_A^4 = I_e(O_a) = I_F\left(\frac{1}{2} + \frac{3}{4} O_a\right) \qquad (3.40)$$

Defines the temperature of the atmosphere as a function of optical depth. Substituting (3.40) at O_{ab} into (3.38) obtains the Earth's surface temperature.

$$\sigma T_G^4 = I_e(O_{ab}) + \frac{I_F}{2} = I_F\left(1 + \frac{3}{4} O_a\right) \qquad (3.41)$$

Three things are noteworthy about these last two equations.

(i) The temperature T_G exceeds the value due to absorbing solar radiation directly (= I_F) as long as the atmosphere absorbs some radiation since the atmospheric absorption is given by the optical depth.

(ii) There is a discontinuity between the atmospheric temperature at the base of the atmosphere and the ground temperature in this model.

(iii) Since there is a net upward flux, then $E_U > E_D$ and that requires the temperature to be greater below than above at *every* level. To have a stratosphere, where temperature is isothermal or increases with elevation, then another process is needed, specifically, absorption of solar radiation by an atmospheric constituent.

If the absorber has a simple exponential variation with elevation, then one obtains a comparatively simple T_A profile. Return to Chapter 6 of the original book, equation (6.20)

If the profile of τ is known (including the value at the bottom of the atmosphere, τ_1) then the temperature profile can be found. Goody and Yung (1989) use a simple exponential profile that is proportional to the distribution of *water* vapor (not dry air) density in the atmosphere.

$$O_a(z) = O_1 \exp\left(-\frac{z}{H}\right) \qquad (6.20)$$

where H = 2 km is an appropriate scale height for water vapor according to Goody and Yung (1989). Substituting (6.20) into (6. 18) gives

$$T(z) = \left[\frac{I_F}{2\sigma}\left\{1 + \frac{3}{2} O_1 \exp\left(-\frac{z}{H}\right)\right\}\right]^{\frac{1}{4}} \qquad (6.21)$$

Before temperature profiles, skin temperatures, and surface temperatures may be estimated, one needs to know O_1 and I_F. For radiative equilibrium, the solar energy absorbed by the earth must balance that lost to space by infrared emission. The solar flux received at the earth's average orbital distance from the sun is I_{sol} = 1380 W m^{-2}. The use of daily averages of the insolation

(Q_o/24) is reasonable since the radiative cooling rates are small (a few degrees per day, Bernstein et al., 1996) compared to the range of temperature over the depth of the troposphere (or as seen in the figure of [T]). The average earth albedo (Figure 3.7) is A = 0.31. If I_{Fa} is the solar energy absorbed, then for energy balance the skin temperature is

$$T_s = \left(\frac{I_{Fa}}{2\sigma}\right)^{\frac{1}{4}} = \left(\frac{I_{sol}[1-A]}{8\sigma}\right)^{\frac{1}{4}} = 214\text{K} \quad (6.22)$$

where the factor of four in the denominator arises because the solar flux hits the cross-sectional disk of the earth (πr_e^2 where r_e is the earth's radius) but the emission is assumed uniformly spread over the whole earth's surface $(4\pi r_e^2)$.

Radiative equilibrium temperature profiles are easily calculated from (6. 18) and (6. 19) once the optical depth is known. The optical depth will respond to different absorbers, which have different vertical profiles. Equation (6.20) uses an exponential variation of water vapor. In contrast, naturally occuring ozone has highest concentrations in the middle stratosphere. Figure 6.2a approximates the ozone profile with a simple function

$$\rho_{o_3} = Bz^2 \exp(az) \qquad (6.23)$$

The corresponding optical depth, due only to ozone, is

$$O_{o_3} = \frac{kB}{a}\left(2\frac{z}{a} - z^2 - \frac{2}{a^2}\right)\exp(az) \qquad (6.24)$$

Radiative equilibrium profiles for the ozone and water vapor absorptions, separately and together, are illustrated in Figure 6.2.

The solutions asymptotically approach 214 K as $O_a \rightarrow 0$ (Figure 6.2b, dashed line). For $O_a \rightarrow 0$ the atmosphere is nearly transparent and is isothermal at the skin temperature; the ground temperature is 40.5 K larger.

For water vapor, the equilibrium temperature profile follows the skin temperature in the high atmosphere because there is no vapor there. At low levels the temperature changes rapidly with height (Figure 6.2b, solid line). The temperature discontinuity at the bottom is 23.6 K. The rate of change of temperature with height increases as z decreases and increases for larger values of O_1. Near the surface, the lapse rate rapidly increases with τ; that diminishes the temperature discontinuity at the same time. Goody and Yung (1989) make a similar calculation and find the discontinuity between surface and air temperatures to be 11.3 K for O_1 = 4, but 16.7 K for O_1 = 2. The lapse rates near the surface become so large that they exceed the dry adiabatic lapse rate when O_1 is greater than about 0.5. Obviously, such convectively unstable lapse rates are another unrealistic feature of a radiative equilibrium model. Superadiabatic lapse rates are partly a reflection of the sharp exponential increase of the water vapor (2 km scale height).

The ozone profile chosen has a smoother variation with height (8 km scale height). The ozone profile does not develop superadiabatic lapse rates (Figure 6.2b, dot-dashed line). Because the ozone concentration diminishes rapidly in the troposphere, the optical depth does not change much either. Consequently, the equilibrium temperature profile does not change much in the troposphere. The surface temperature discontinuity is 27.8 K.

When the ozone and water vapor absorptions are combined (dotted line), the result exhibits properties of both absorbers. In these calculations solar absorbtion is absent. Ozone is an effective absorber of solar radiation in the middle atmosphere. Incorporation of that effect can lead to increasing temperature with height in the lower stratosphere, a feature not present in Figure 6.2b.

As mentioned above, the two main unrealistic features of the radiative equilibrium model are (1) the development of superadiabatic lapse rates near the ground and (2) the temperature discontinuity at the ground. The second model introduces convective adjustment to eliminate both of these problems. Such a model is called a radiative-convective model. The common approach has been to specify a lapse rate from the surface up to a height z_t, the model's "tropopause." Using average conditions over the earth, then T is given by (6.21) in the model's "stratosphere" above z_t and by

$$\mathrm{T}(z) = \mathrm{T}(z_t) + \Gamma(z_t - z) \qquad (6.25)$$

in the troposphere. The tropospheric lapse rate may be specified to be several values. A constant lapse rate $\Gamma = 6.5$ K km^{-1} is used in Figure 6.2c (the dashed lines). Near the surface, this lapse rate would be similar to the moist adiabatic lapse rate for typical middle latitude conditions. The actual moist adiabatic lapse rate varies with the moisture content of the air; it can be as little as 3 K km^{-1} near the surface in the tropics and approaches the dry adiabatic rate (9.8 K km^{-1}) in the upper atmosphere.

The radiation flux is no longer constant in the model troposphere, so that equation (6. 11) must be used instead of (6. 12). In addition, the convective layer extends higher than the level at which the radiative temperature profile (6.21) has lapse rate equal to Γ (dot-dashed line in Figure 6.2c). This occurs because the flux at the top of the convective layer must match the radiative equilibrium flux I_F in the stratosphere. If the dot-dashed profile in Figure 6.2c is used, the temperature in the troposphere is everywhere less than the radiative equilibrium profile, hence the flux out of the troposphere would be too small. Even so, the surface temperatures can be greatly reduced by the convection. The resulting temperature profile is similar to observed annual average temperature. Of course part of the agreement is built in by using a value of Γ that is similar to the observed lapse rate. Needless to say, the height of the tropopause is not specified, but is derived and is comparable to observed heights (Figure 3.11).

A pair of papers (Manabe and Strickler, 1964; Manabe and Wetherald, 1967) introduce several further modifications to the radiative-convective model. Their model differs from that just shown in the following ways: (a) a specific latitude (35 N), time of year (April), and local albedo (0.102) are used; (b) observed profiles of H_2O, O_3, and CO_2 are employed; and (c) the atmosphere is allowed to absorb solar radiation. As is seen in Figure 6.3, the model arrives at the equilibrium profile by iteration. Isothermal profiles are assumed at the start and the lapse rates are adjusted so as never to exceed $\Gamma = 6.5$ K km^{-1}. The radiative and radiative-convective models have one obvious difference from before. Temperature now increases with height in the stratosphere; the effect is created primarily by the O_3 absorption of the solar radiation (Figure 3.2 or 3.3a) mentioned earlier in this section.

Discussion of Ozone heating that changes I_F to depend on O_a as in course notes. I_F decrease as optical depth increases (as elevation becomes lower) makes intuitive sense since shortwave radiation is being absorbed and therefore less reaches the levels below, including the Earth's surface. Such a change is consistent with calculations made from ISCCP data (Zhang et al., 2004).

Further refinements have been made to these types of models. For example, the specification of the tropospheric lapse rate can be avoided by use of a convection model. Using such a model makes sense since the dry adiabatic lapse rate is steeper than 6.5 K/km. Lindzen et al. (1982), for example, make this refinement and predict the Γ profile with moist and dry convection models. Clouds have a complex effect upon the temperature profile. Figure 6.4 shows results from Liou and Ou (1983), whose model includes a convective model, water vapor, ozone, and clouds. They find, as in previous studies with clouds (e.g., Manabe and Strickler, 1964), that middle clouds reduce the temperatures throughout the troposphere and lower stratosphere. Low clouds reduce the temperatures even more. In contrast, high clouds (located just below or even above the tropopause) can increase the temperatures throughout the troposphere. The net effect varies with cloud altitude because of two competing effects. First, clouds reflect solar radiation (a cooling effect). Second, clouds can trap infrared terrestrial radiation (a heating effect). Because the cloud is opaque, it absorbs nearly all the radiation emitted from the earth's surface; the trapping occurs because the typical cloud emits less radiation to space than does the earth's surface because the cloud is cooler. The first effect, the reflection effect, dominates for low and middle clouds. For high clouds, their temperature is so low that the second effect, the trapping effect, dominates. Clouds occur at many elevations in the atmosphere. On a global average, the cooling effect from reflection dominates, according to satellite observations (e.g., Rossow and Schiffer, 1991).

However, in the tropics the heating and cooling are very large but nearly canceling. The global average cloud cooling is largely due to middle latitude clouds.

Convection is a vertical transport of heat. Another refinement is to incorporate the *horizontal* transports of heat in the atmosphere. These transports are expected from the net radiation curves described in §3.1. Liou and Ou (1983) compare solutions from two types of models. The temperature profiles obtained by their one-dimensional model (using climatological cloud distributions that vary with latitude) are plotted as the dashed lines in Figure 6.5. To improve the simulation, horizontal heat transports between three latitudinal belts are incorporated by Liou and Ou (1983) in their "two-dimensional" model. (The observed transport of sensible heat may be estimated by multiplying the field plotted in Figure 4.31 by C_p and atmospheric density.) The heat transport is poleward for the three belts. Below about 4 km the transport into the midlatitude belt from the tropics exceeds the transport out, towards the polar belt. Higher up, the transport out to the polar belt slightly exceeds the input from the tropical belt. One can anticipate the following changes: the net transport out of the tropics will lower the tropospheric temperatures in that belt; net convergence in the polar belt and in midlatitudes (below 4 km) will raise the temperatures in those belts. These changes appear in Figure 6.5 (dotted lines).

Several other refinements have been made to radiative-convective models. More recent uses of the models focus on the study of "greenhouse" gases (e.g., Ramanathan et al., 1987). Changes in the concentrations of these trace gases are inserted and new temperature profiles calculated. A very different application is by Held (1982), who attempted to relate the height of the tropopause to the baroclinic instability of the flow (§7.1). He used a simple radiative-convective model with fixed tropospheric lapse rate. A marginally baroclinically unstable flow will have a certain ratio of horizontal to vertical temperature gradients. The degree of instability varies with Coriolis parameter as well as vertical shear. By exploiting these connections he obtained a tropopause that decreased with increasing latitude. Figure 3.5 shows such a decrease.

A class of simple models exists for investigating surface temperature. Energy balance climate models (EBMs) simulate surface temperature for various, mainly climate change, scenarios (e.g., North, 1975). An EBM balances input and output of radiation at the surface. The solar flux is multiplied by an albedo that is dependent in some *empirical* way on temperature (T) and latitude φ. Terrestrial emission depends upon T^4 from the Stefan-Boltzmann law, and also upon an empirical coefficient that depends upon T and φ, too. The models have time-dependent temperature except when input and output match. The matches are equilibrium temperatures: three, five, or more matches are found in the EBM, but usually just two are stable states. One stable state matches the observed temperature distribution if the empirical factors are properly chosen. A second stable state corresponds to an ice-covered earth.

Before leaving this section, it is instructive to introduce some properties of the stratosphere. Here, local radiative balance was first proposed to explain the stratospheric temperatures, with convection invoked in the troposphere. With some embellishment from horizontal heat fluxes, calculated temperature profiles can reflect the observed latitudinal differences. Those heat fluxes are necessary not just because the incoming radiation (Figure 3.6) has a greater latitudinal variation than the outgoing radiation. Local radiative balance may not be compatible with a balanced circulation. For example, Shine (1987) shows that equilibrium temperature fields in other seasons do not have solutions able to satisfy gradient wind balance. According to McIntyre (1987), the summer hemisphere radiative equilibrium temperature field is balanced only by a very strong *surface* circumpolar vortex. Nonetheless, radiative equilibrium gives a good approximation to the stratospheric temperatures. One consequence is that stratospheric temperatures respond to solar radiation more directly than do tropospheric temperatures. The troposphere is quite sensitive to earth surface temperatures, which take more time to warm up (or cool down) as summer (or winter) arrives. In addition, the stratosphere contains few clouds, whose seasonal changes partially oppose the seasonal changes in radiation (Figure 3.7). However, the much-publicized “ozone hole” above the South Pole illustrates that the radiatively active constituents can vary greatly from place to place and over time in one locale. Even so, the seasonal changes of tropospheric weather lag the solar cycle by about a month, but little lag is apparent in stratospheric data (e.g., Geller and Wu, 1987).

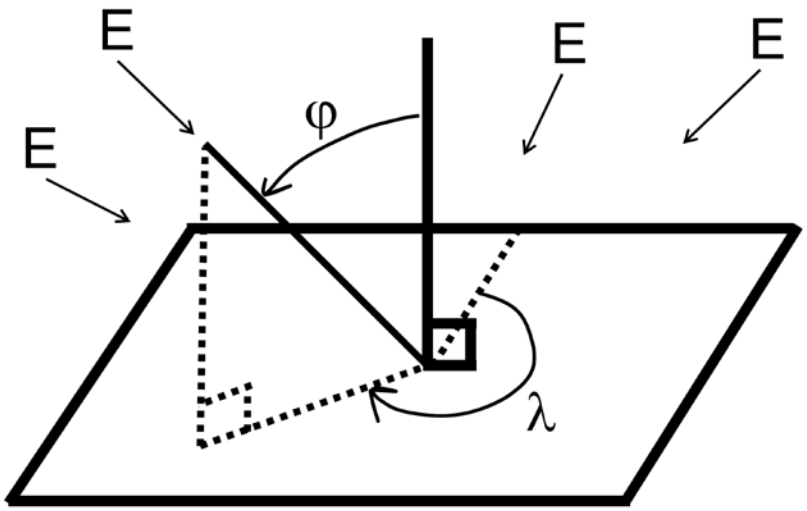

Figure 3.1

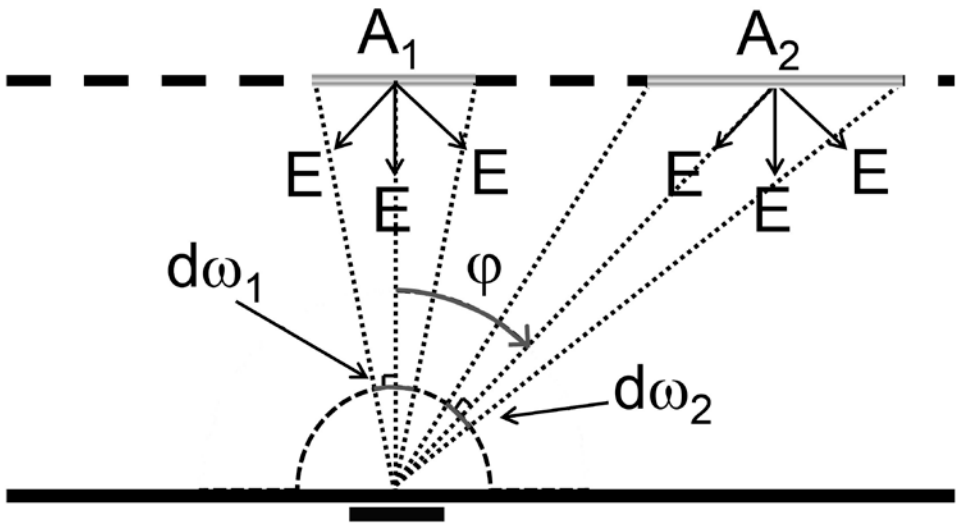

Figure 3.2

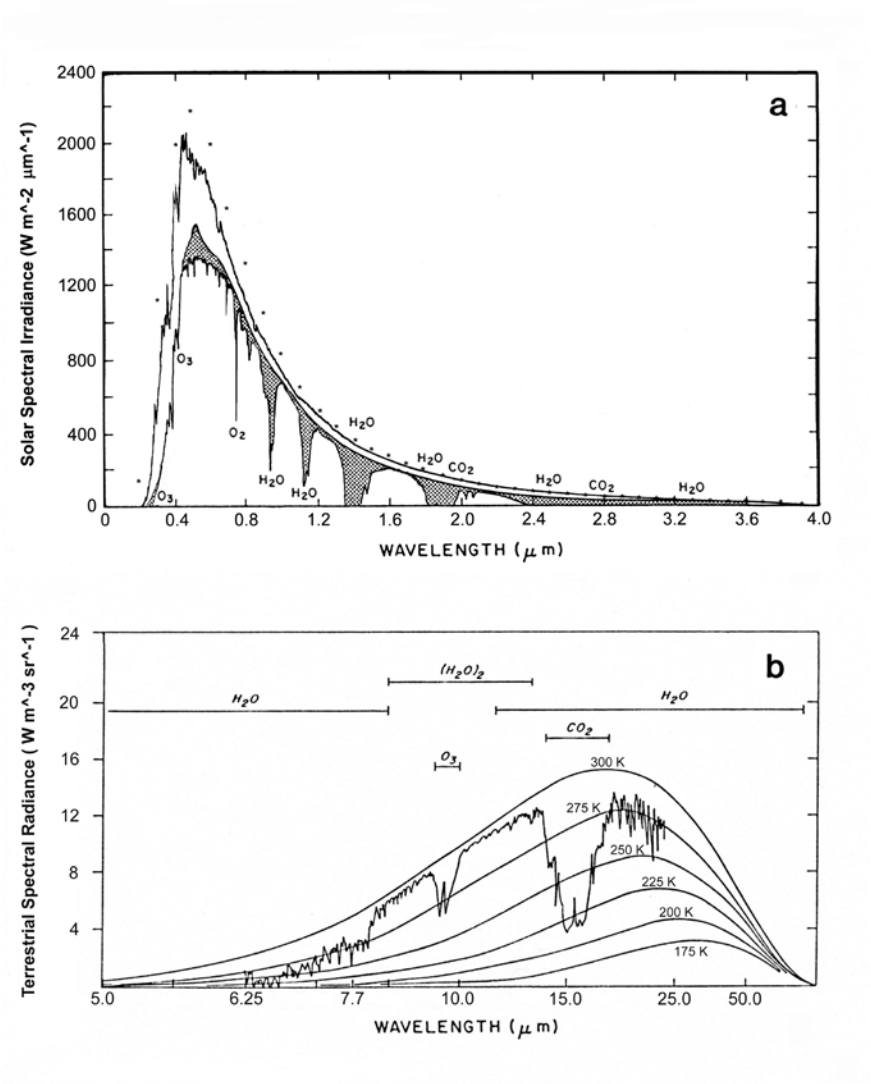

Figure 3.3 (a) Solar spectral irradiance (shortwave radiation) .. Top of atmosphere (TOA) and surface spectral values based on data provided by R. Rohde (2007; http://www.globalwarmingart.com/wiki/File:Solar_Spectrum_png) .. Shaded area estimates the terrestrial absorption based on Thekaekara (1976). Asterisks are point values for spectral irradiance at the Earth's orbit if the sun were a 6000K black body. (b) Terrestrial radiation for a region of the subtropical Pacific measured by a polar orbiting satellite as it passed over Guam. This panel redrawn from data in Liou (1980). The abscissa is equally-spaced in wavenumber, but stretched in wavelength.

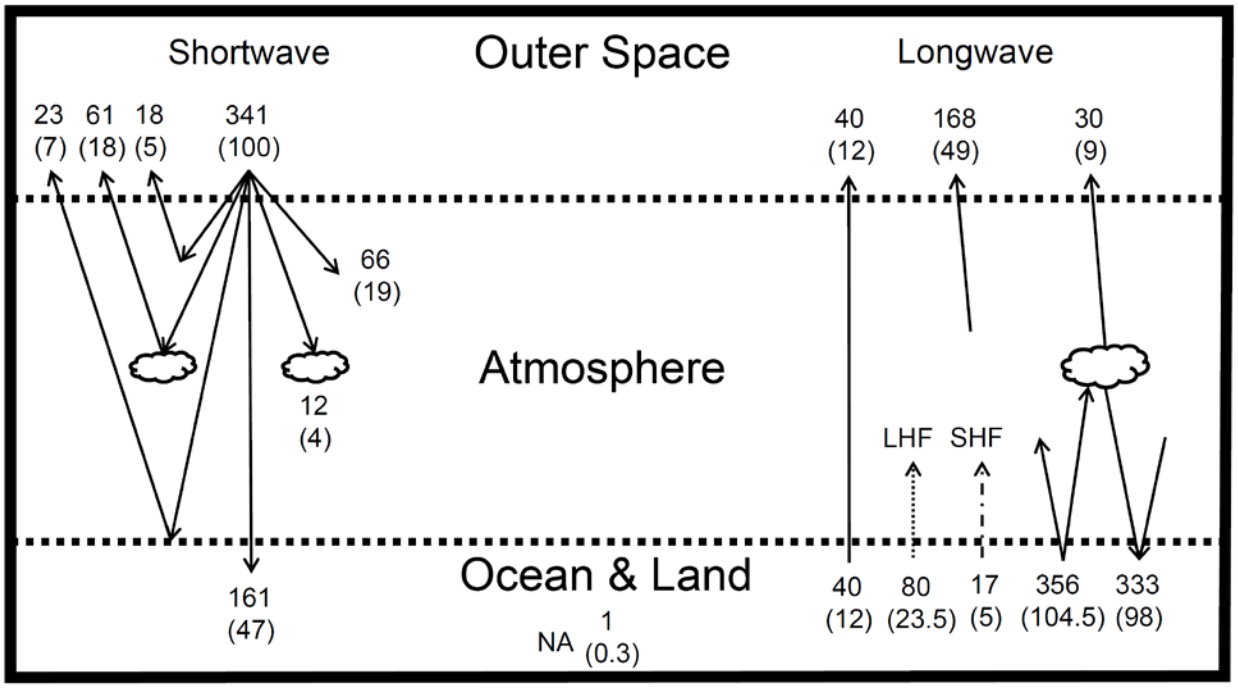

Figure 3.4 Estimates of major components of the global energy balance based upon data in Trenberth et al. (2009) with adjustments in Grotjahn (1993). Two numbers are presented, with the top number in units of W/m^2 while the number in parentheses is the corresponding percentage of the incoming radiation. Abbreviations: LHF is latent heat flux from the Earth's surface; SHF is sensible heat flux from the Earth's surface; NA is net absorption by the Earth system (ocean, land, atmosphere) as estimated by Hansen et al. (2005).

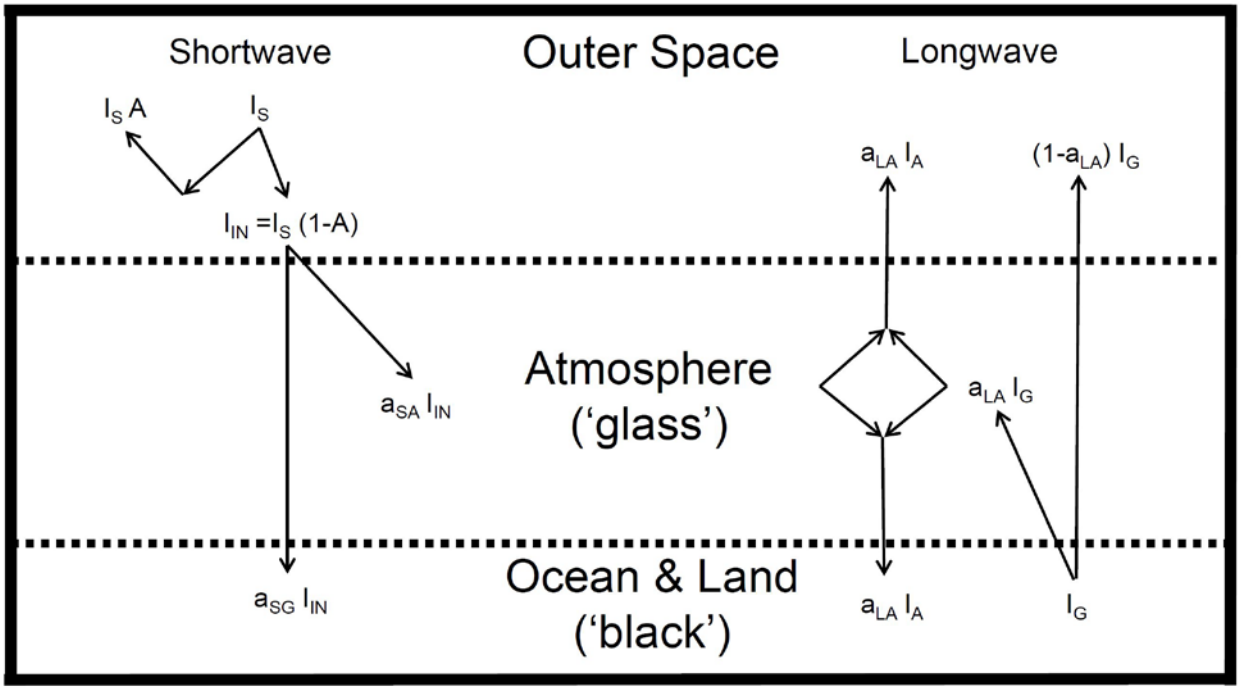

Figure 3.5 Parameters for the 'glass slab' model of radiative balance for the global atmosphere.

Fig. 3.6 (iterative model)

Fig. 3.7 (shortwave radiative components – zonally averaged, annual + 2 extreme seasons)

Fig. 3.8 (longwave radiative components – zonally averaged, annual + 2 extreme seasons)

Fig. 3.9 (zonal variations of shortwave, longwave, net radiation)

Fig. 3.10 (zonal and time mean heat transports)

Fig. 3.11 ($[v\theta]$ in diff seasons)

Fig. 3.12 (schematic of vLq)

Fig. 3.13 ([T] different extreme seasons)

Fig. 3.14 (SH vs NH T differences)

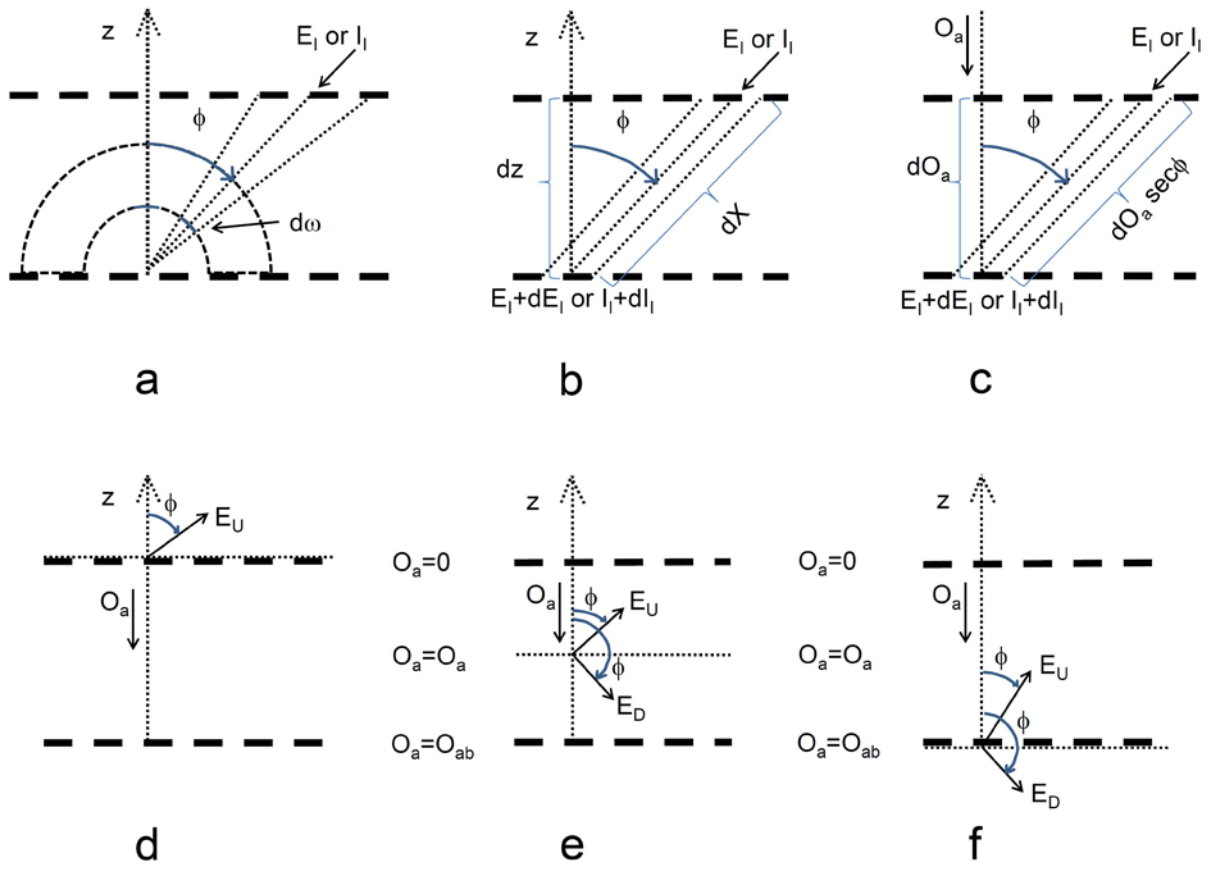

Figure 3.15. Geometry and notation used by the radiative-equilibrium and radiative-convective models.